

Supporting Information

A Structurally Flexible Triazolate-Based Metal-Organic Framework Featuring Coordinatively Unsaturated Copper (I) Sites

Phillip Schmieder,^a Dmytro Denysenko,^a Maciej Grzywa,^a O. Magdysyuk^b and Dirk Volkmer*^a

^a Institute of Physics, Chair of Solid State and Material Science, Augsburg University,
D-86135 Augsburg, Germany. E-mail: dirk.volkmmer@physik.uni-augsburg.de;
Fax: (+)49 (0)821 598-5955

^b O. Magdysyuk, Diamond Light Source Ltd., Harwell Science and Innovation Campus, Didcot, Oxfordshire, OX11
ODE (United Kingdom)

Contents

1. IR spectroscopy
2. Gas sorption measurements
3. Catalysis with CFA-8
4. Selected bond lengths and angles for the large-pore phase of CFA-8
5. Le Bail fit of activated phase of CFA-8
6. Single crystal measurement of the narrow-pore phase of CFA-8
7. UV/vis spectroscopy
8. Variable temperature synchrotron powder diffraction measurements
9. Structure solution and refinement from powder diffraction data of the
narrow-pore phase of CFA-8 with adsorbed CO molecules
10. In situ XRPD measurements under CO₂ and 80 % humidity

1. IR spectroscopy

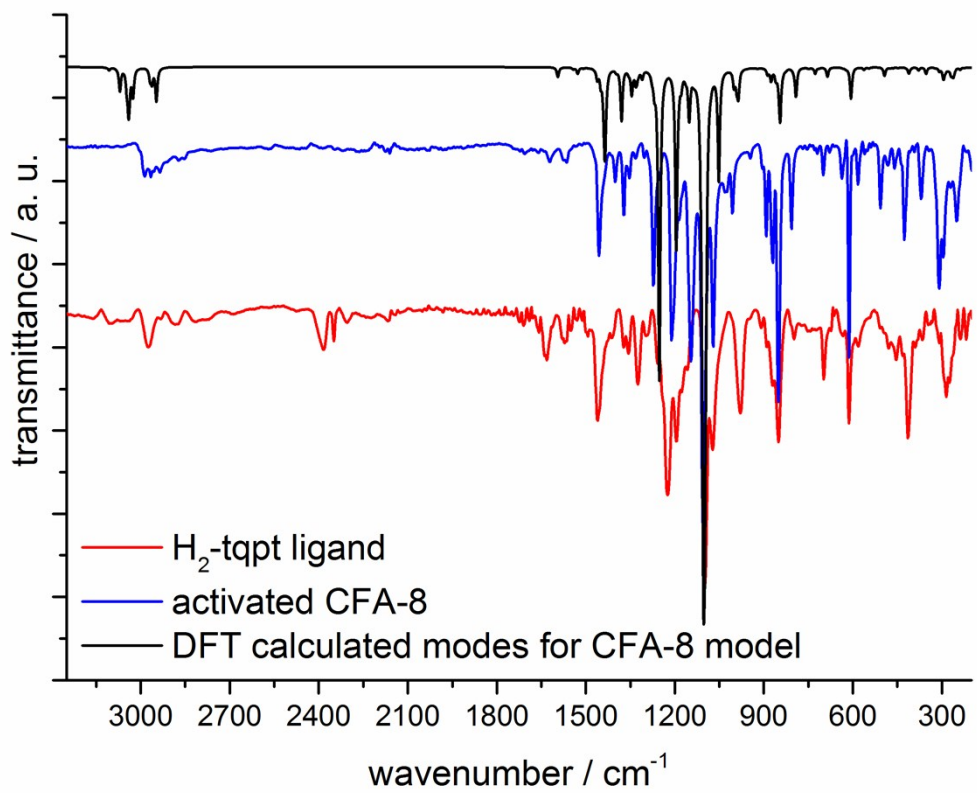


Figure S 1 IR spectra of CFA-8 (blue); the organic ligand H₂-tqpt (red) and the DFT calculated IR spectra for CFA-8 (black).

2. Gas sorption measurements

The isosteric heats of adsorption were calculated from the measured isotherms (Figure S 2, Figure S 3) using the Clausius-Clapeyron equation (I). The slopes of linear plots $\ln P$ versus $1/RT$ for different loadings (Figure S 4, Figure S 5) give the adsorption enthalpies, according to the equation (II).

$$Q_{st} = -R \left(\frac{\partial(\ln P)}{\partial(1/T)} \right)_{\theta} \quad (\text{I}), \Theta - \text{surface coverage}$$

$$\ln P = -\frac{Q_{st}}{R} \left(\frac{1}{T} \right) + C \quad (\text{II}), C - \text{integration constant}$$

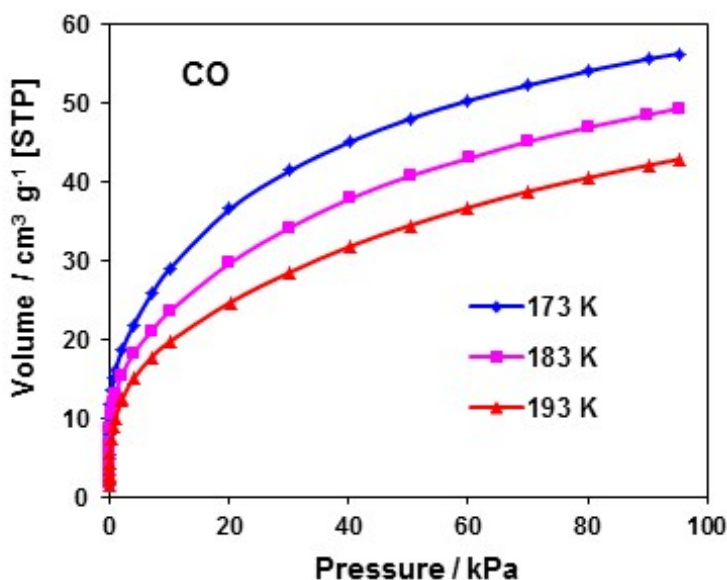


Figure S 2 CO adsorption isotherms for CFA-8 at different temperatures for the determination of the isosteric heat of adsorption.

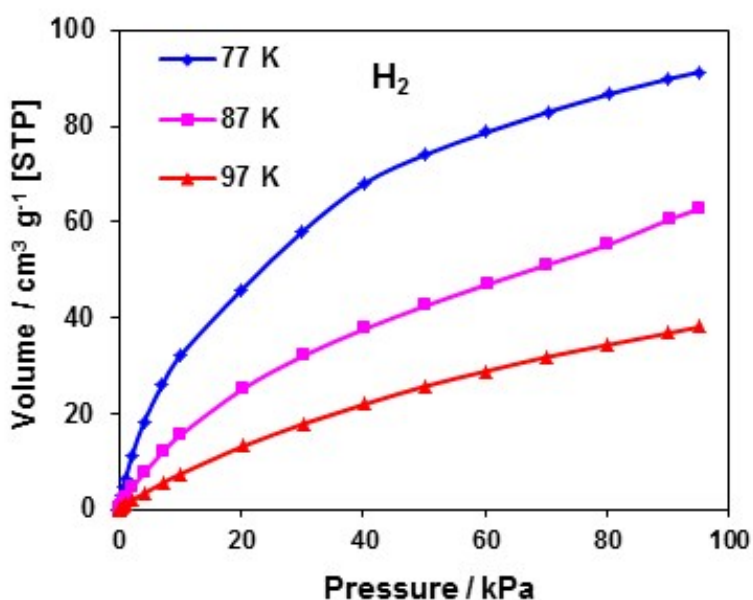


Figure S 3 H₂ adsorption isotherms for CFA-8 at different temperatures for the determination of the isosteric heat of adsorption.

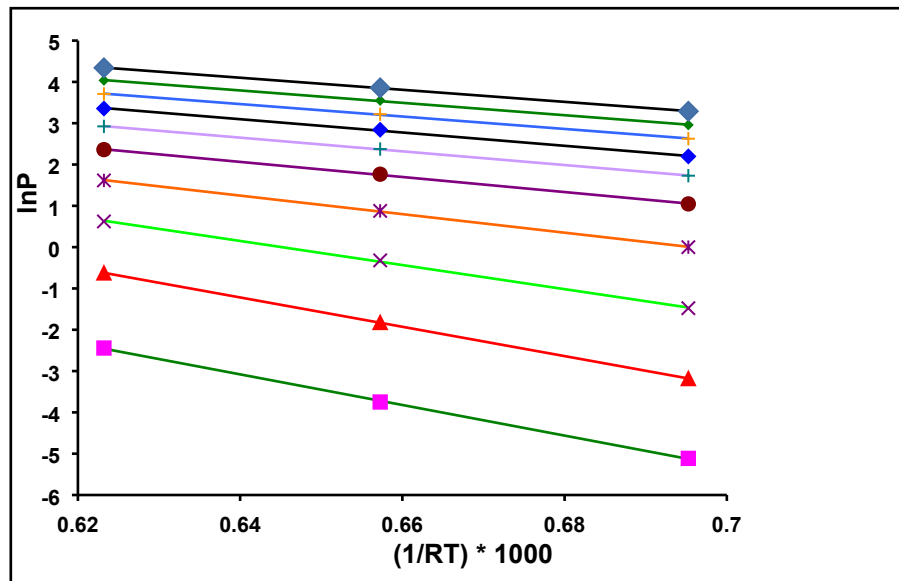


Figure S 4 $\ln P$ versus $1/RT$ plots for different loadings for CO adsorption on CFA-8.

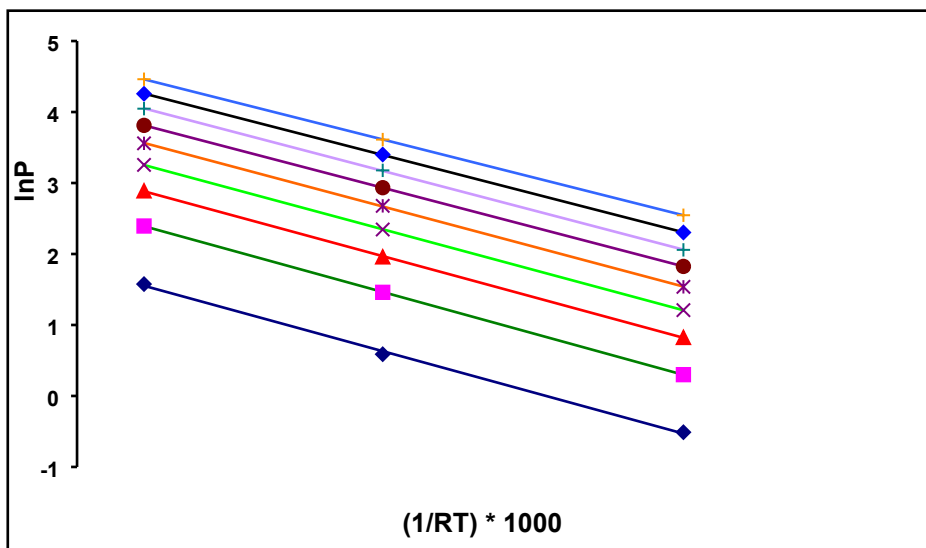
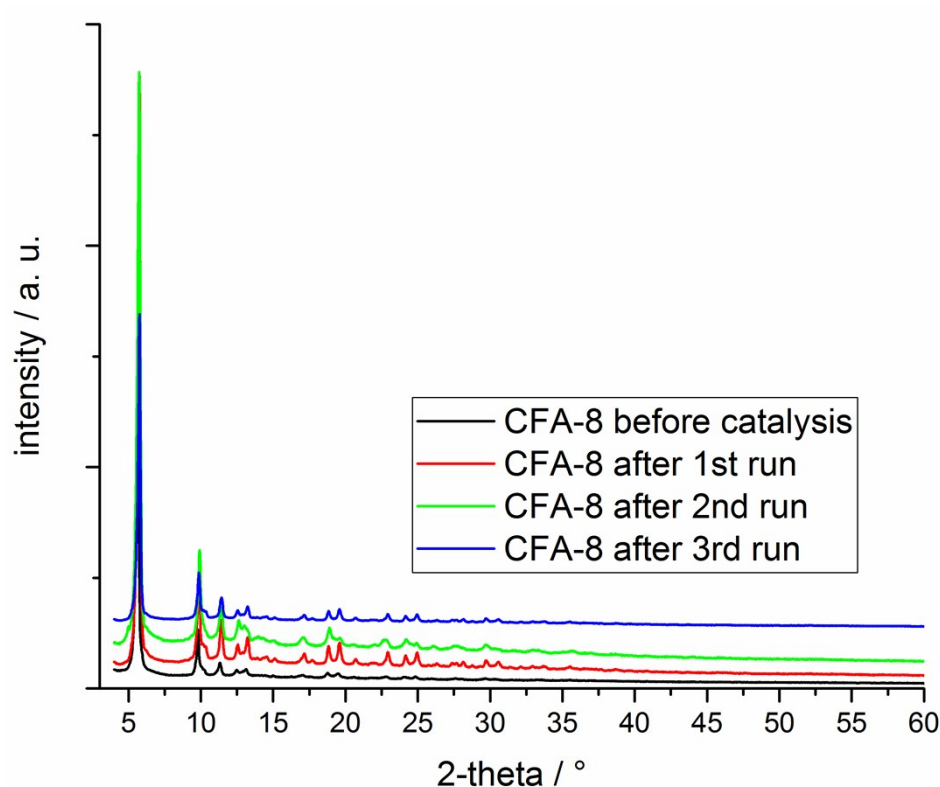
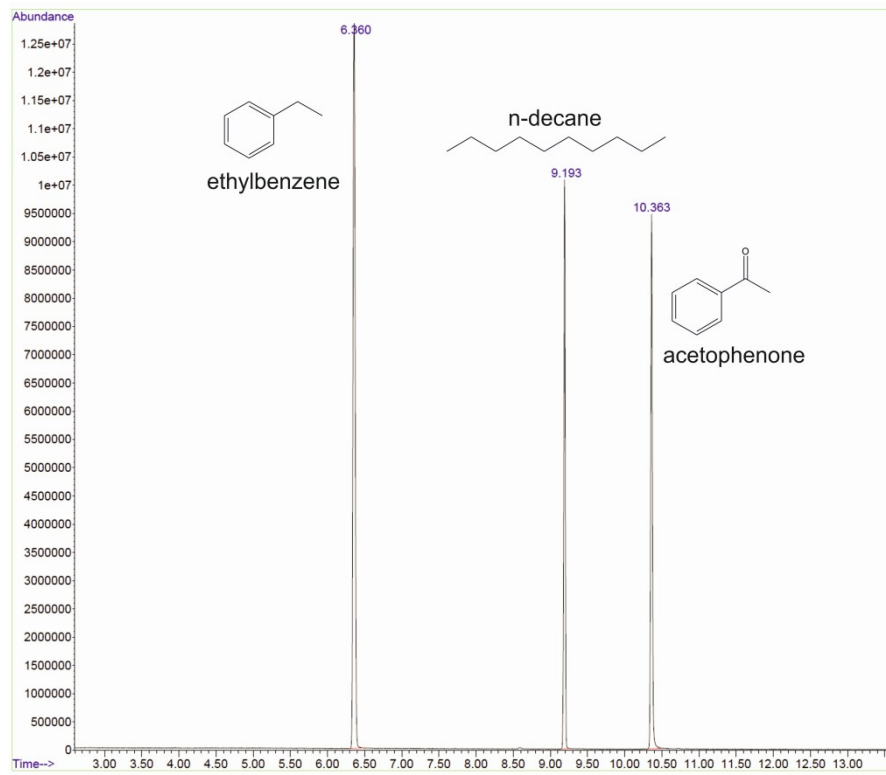


Figure S 5 $\ln P$ versus $1/RT$ plots for different loadings for H_2 adsorption on CFA-8.

Table S1: loading-dependent isosteric heats of CO and H_2 adsorption in CFA-8 (kJ mol^{-1} ; errors are standard deviations calculated for the linear regression).

Loading / $\text{cm}^3 \text{g}^{-1}$ [STP]	CO	H_2
4	37.1 ± 0.7	6.5 ± 0.2
8	35.5 ± 0.2	6.50 ± 0.03
12	29.2 ± 0.8	6.41 ± 0.06
16	22.4 ± 0.4	6.35 ± 0.02
20	18.3 ± 0.4	6.28 ± 0.05
24	16.6 ± 0.3	6.17 ± 0.01
28	16.1 ± 0.6	6.18 ± 0.04
32	15.1 ± 0.4	6.07 ± 0.03
36	15.0 ± 0.4	5.95 ± 0.01
40	14.6 ± 0.2	-

3. Catalysis with CFA-8



4. Selected bond lengths and angles for the large-pore phase of CFA-8

Table S2: Bond lengths [\AA] and angles [$^\circ$] for the large-pore phase of CFA-8

bond	length [\AA]	atoms	angle [$^\circ$]
Cu(1)-N(1)	1.931(3)	N(1)-Cu(1)-N(3)#1	131.78(12)
Cu(1)-N(3)#1	1.935(3)	N(1)-Cu(1)-N(9)#2	113.25(11)
Cu(1)-N(9)#2	1.995(3)	N(3)#1-Cu(1)-N(9)#2	114.92(12)
N(1)-N(2)	1.349(4)	N(2)-N(1)-C(1)	105.8(3)
N(1)-C(1)	1.367(4)	N(2)-N(1)-Cu(1)	123.4(2)
C(1)-C(6)	1.379(5)	C(1)-N(1)-Cu(1)	130.8(2)
C(1)-C(2)	1.419(5)	N(1)-C(1)-C(6)	130.8(3)
Cu(2)-N(2)#3	2.008(3)	N(1)-C(1)-C(2)	107.6(3)
Cu(2)-N(2)	2.008(3)	C(6)-C(1)-C(2)	121.6(3)
Cu(2)-N(8)#4	2.027(3)	N(2)#3-Cu(2)-N(2)	116.84(15)
Cu(2)-N(8)#2	2.027(3)	N(2)#3-Cu(2)-N(8)#4	108.28(11)
N(2)-N(3)	1.320(4)	N(2)-Cu(2)-N(8)#4	107.21(11)
C(2)-N(3)	1.374(4)	N(2)#3-Cu(2)-N(8)#2	107.21(11)
C(2)-C(3)	1.376(5)	N(2)-Cu(2)-N(8)#2	108.27(11)
Cu(3)-N(10)	1.874(3)	N(8)#4-Cu(2)-N(8)#2	108.85(16)
Cu(3)-N(10)#5	1.874(3)	N(3)-N(2)-N(1)	113.1(2)
N(3)-Cu(1)#6	1.935(3)	N(3)-N(2)-Cu(2)	121.4(2)
C(3)-C(4)	1.406(5)	N(1)-N(2)-Cu(2)	125.5(2)
N(4)-C(7)	1.314(4)	N(3)-C(2)-C(3)	130.9(3)
N(4)-C(4)	1.380(5)	N(3)-C(2)-C(1)	106.7(3)
C(4)-C(5)	1.438(5)	C(3)-C(2)-C(1)	122.3(3)
N(5)-C(12)	1.306(5)	N(10)-Cu(3)-N(10)#5	178.45(18)
N(5)-C(5)	1.374(4)	N(2)-N(3)-C(2)	106.7(3)
C(5)-C(6)	1.396(5)	N(2)-N(3)-Cu(1)#6	119.8(2)
N(6)-C(9)	1.317(5)	C(2)-N(3)-Cu(1)#6	133.3(2)
N(6)-C(17)	1.399(4)	C(2)-C(3)-C(4)	116.9(3)
N(7)-C(10)	1.310(4)	C(7)-N(4)-C(4)	118.6(3)
N(7)-C(22)	1.374(5)	N(4)-C(4)-C(3)	119.2(3)
C(7)-C(12)	1.447(5)	N(4)-C(4)-C(5)	120.0(3)
C(7)-C(8)	1.514(5)	C(3)-C(4)-C(5)	120.7(3)
N(8)-N(9)	1.310(4)	C(12)-N(5)-C(5)	118.6(3)
N(8)-C(19)	1.392(4)	N(5)-C(5)-C(6)	119.1(3)
N(8)-Cu(2)#7	2.027(3)	N(5)-C(5)-C(4)	119.8(3)
C(8)-C(14)	1.527(6)	C(6)-C(5)-C(4)	121.1(3)
C(8)-C(9)	1.530(5)	C(9)-N(6)-C(17)	118.0(3)
C(8)-C(13)	1.546(5)	C(1)-C(6)-C(5)	117.3(3)
N(9)-N(10)	1.342(4)	C(10)-N(7)-C(22)	118.4(3)
N(9)-Cu(1)#7	1.995(3)	N(4)-C(7)-C(12)	120.8(3)
C(9)-C(10)	1.449(5)	N(4)-C(7)-C(8)	117.3(3)
N(10)-C(20)	1.380(4)	C(12)-C(7)-C(8)	121.8(3)
C(10)-C(11)	1.510(5)	N(9)-N(8)-C(19)	107.1(3)
C(11)-C(15)	1.517(6)	N(9)-N(8)-Cu(2)#7	125.3(2)

C(11)-C(16)	1.528(6)	C(19)-N(8)-Cu(2)#7	127.3(2)
C(11)-C(12)	1.532(5)	C(7)-C(8)-C(14)	107.1(3)
C(17)-C(18)	1.368(5)	C(7)-C(8)-C(9)	111.6(3)
C(17)-C(22)	1.436(5)	C(14)-C(8)-C(9)	107.0(3)
C(18)-C(19)	1.399(5)	C(7)-C(8)-C(13)	111.1(3)
C(19)-C(20)	1.407(5)	C(14)-C(8)-C(13)	109.3(4)
C(20)-C(21)	1.389(5)	C(9)-C(8)-C(13)	110.5(3)
C(21)-C(22)	1.397(5)	N(8)-N(9)-N(10)	112.8(3)
		N(8)-N(9)-Cu(1)#7	122.9(2)
		N(10)-N(9)-Cu(1)#7	124.1(2)
		N(6)-C(9)-C(10)	121.8(3)
		N(6)-C(9)-C(8)	117.2(3)
		C(10)-C(9)-C(8)	120.8(3)
		N(9)-N(10)-C(20)	106.4(3)
		N(9)-N(10)-Cu(3)	123.5(2)
		C(20)-N(10)-Cu(3)	130.1(2)
		N(7)-C(10)-C(9)	121.5(3)
		N(7)-C(10)-C(11)	114.7(3)
		C(9)-C(10)-C(11)	123.8(3)
		C(10)-C(11)-C(15)	109.9(3)
		C(10)-C(11)-C(16)	108.7(4)
		C(15)-C(11)-C(16)	109.6(4)
		C(10)-C(11)-C(12)	111.6(3)
		C(15)-C(11)-C(12)	108.9(3)
		C(16)-C(11)-C(12)	108.1(3)
		N(5)-C(12)-C(7)	122.0(3)
		N(5)-C(12)-C(11)	115.4(3)
		C(7)-C(12)-C(11)	122.7(3)
		C(18)-C(17)-N(6)	118.3(3)
		C(18)-C(17)-C(22)	122.4(3)
		N(6)-C(17)-C(22)	119.3(3)
		C(17)-C(18)-C(19)	115.6(3)
		N(8)-C(19)-C(18)	130.9(3)
		N(8)-C(19)-C(20)	106.5(3)
		C(18)-C(19)-C(20)	122.6(3)
		N(10)-C(20)-C(21)	130.6(3)
		N(10)-C(20)-C(19)	107.2(3)
		C(21)-C(20)-C(19)	122.2(3)
		C(20)-C(21)-C(22)	115.6(3)
		N(7)-C(22)-C(21)	117.4(3)
		N(7)-C(22)-C(17)	121.0(3)
		C(21)-C(22)-C(17)	121.6(3)

Symmetry transformations used to generate equivalent atoms:

#1 x,-y+1,z+1/2 #2 x+1/2,y+1/2,z #3 -x+2,y,-z+1/2
#4 -x+3/2,y+1/2,-z+1/2 #5 -x+1,y,-z+3/2 #6 x,-y+1,z-1/2
#7 x-1/2,y-1/2,z

5. Le Bail fit of activated phase of CFA-8

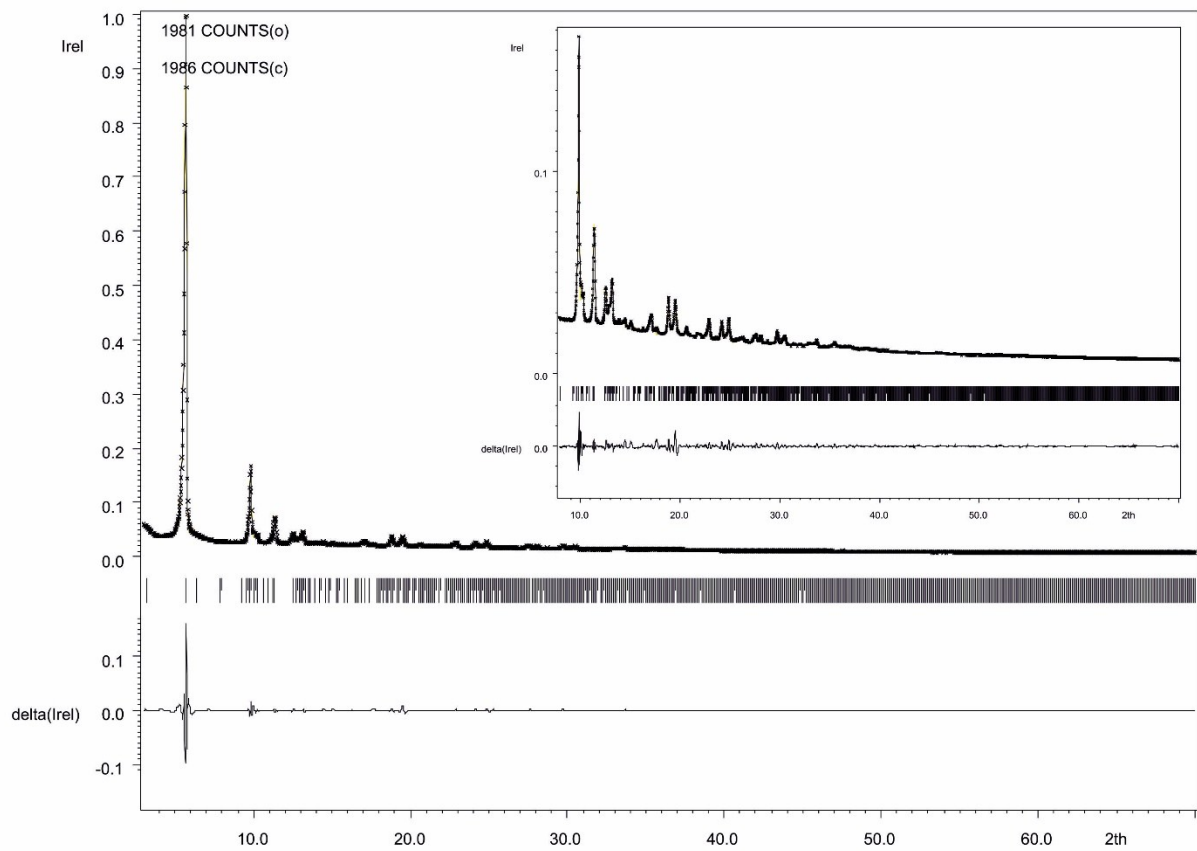


Figure S 8 Le Bail fit of the XRPD pattern of CFA-8 (activated phase). Dotted and solid lines represent observed and calculated patterns, respectively with peak markers and the difference plot shown at the bottom ($R_p = 3.79 \%$, $wR_p = 6.31$).

6. Single crystal measurement of the narrow-pore phase of CFA-8

Table S3: Crystal data and structure refinement for the narrow-pore phase of CFA-8·0.94 P(OCH₃)₃.

	CFA-8·0.94 P(OCH ₃) ₃ , narrow-pore phase
Empirical formula	C _{24.80} H _{24.50} Cu ₂ N ₁₀ O _{2.80} P _{0.94}
Formula weight	663.56
Temperature	100(2) K
Wavelength	0.71073 Å
Crystal system	monoclinic
Space group	C2/c (no. 15)
Unit cell dimensions	a = 32.04(6) Å; α = 90 °; b = 16.79(4) Å; β = 92.36(4) °; c = 10.77(2) Å; γ = 90 °.
Volume	5789(21) Å ³
Z	8
Density (calculated)	1.522 Mg/m ³
Absorption coefficient	1.566 mm ⁻¹
F(000)	2702
Crystal size	0.11 x 0.03 x 0.02 mm ³
Theta range for data collection	2.31 to 25.03°.
Index ranges	-37<=h<=37, -19<=k<=19, -12<=l<=12
Reflections collected	23995
Independent reflections	4967 [R(int) = 0.2206]
Completeness to theta = 25.03°	96.9 %
Refinement method	Full-matrix least-squares on F2
Data / restraints / parameters	4967 / 82 / 312
Goodness-of-fit on F2	1017
Final R indices [I>2sigma(I)]	R1 = 0.0938, wR2 = 0.2007
R indices (all data)	R1 = 0.1876, wR2 = 0.2317
Largest diff. peak and hole	0.835 and -1.231 e.Å ⁻³

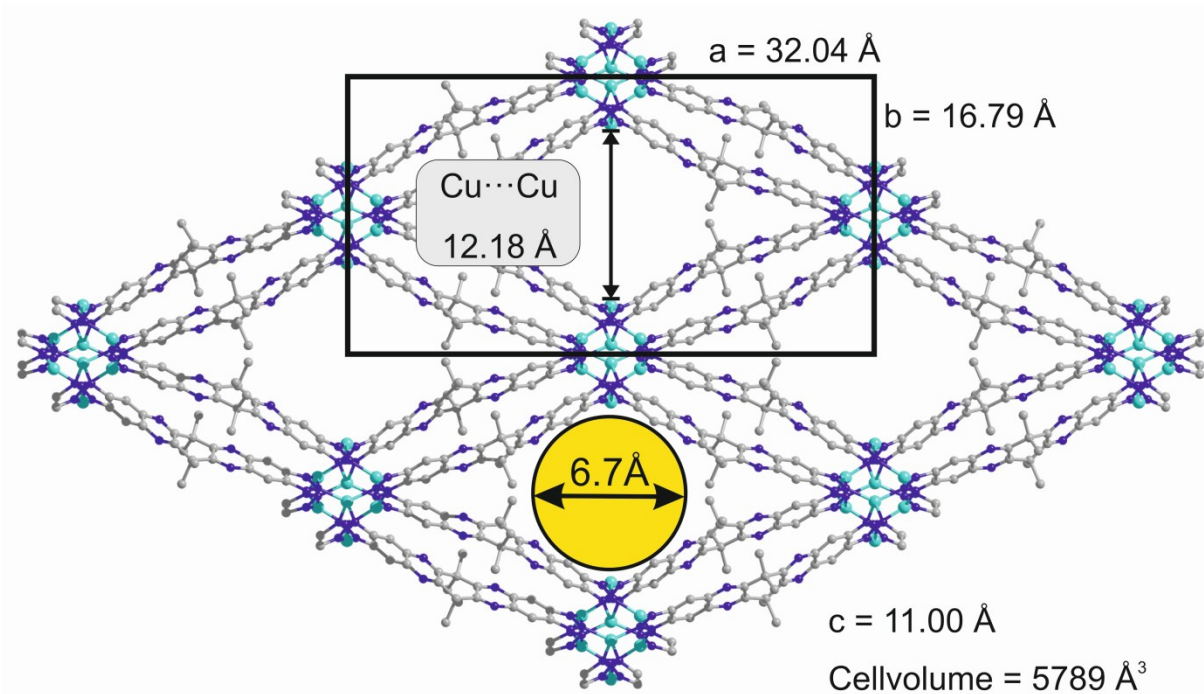


Figure S 9 Ball-and-stick model of the structure solution of the narrow-pore phase of CFA-8.

Table S4: Bond lengths [Å] and angles [°] for the narrow-pore phase of CFA-8.

bond	length [Å]	atoms	angle [°]
Cu(1)-N(2)	2.003(8)	N(2)-Cu(1)-N(2)#1	132.6(4)
Cu(1)-N(2)#1	2.003(8)	N(2)-Cu(1)-N(10)#2	106.5(3)
Cu(1)-N(10)#2	2.065(8)	N(2)#1-Cu(1)-N(10)#2	101.9(3)
Cu(1)-N(10)#3	2.065(8)	N(2)-Cu(1)-N(10)#3	101.9(3)
Cu(2)-N(1)	1.938(8)	N(2)#1-Cu(1)-N(10)#3	106.5(3)
Cu(2)-N(3)#4	1.945(8)	N(10)#2-Cu(1)-N(10)#3	104.8(4)
Cu(2)-N(9)#5	1.987(8)	N(1)-Cu(2)-N(3)#4	127.5(3)
Cu(3)-N(8)	1.877(8)	N(1)-Cu(2)-N(9)#5	118.7(3)
Cu(3)-N(8)#6	1.877(8)	N(3)#4-Cu(2)-N(9)#5	113.7(3)
N(1)-N(2)	1.328(10)	N(8)-Cu(3)-N(8)#6	169.7(5)
N(1)-C(1)	1.378(12)	N(2)-N(1)-C(1)	107.7(7)
N(2)-N(3)	1.329(9)	N(2)-N(1)-Cu(2)	117.0(6)
N(3)-C(2)	1.382(12)	C(1)-N(1)-Cu(2)	134.0(7)
N(3)-Cu(2)#7	1.945(8)	N(1)-N(2)-N(3)	112.4(7)
N(4)-C(7)	1.302(13)	N(1)-N(2)-Cu(1)	120.7(5)
N(4)-C(5)	1.388(12)	N(3)-N(2)-Cu(1)	126.6(6)
N(5)-C(8)	1.332(12)	N(2)-N(3)-C(2)	107.6(7)
N(5)-C(4)	1.375(12)	N(2)-N(3)-Cu(2)#7	123.7(6)
N(6)-C(10)	1.302(13)	C(2)-N(3)-Cu(2)#7	128.7(6)
N(6)-C(16)	1.374(12)	C(7)-N(4)-C(5)	117.9(9)
N(7)-C(11)	1.305(12)	C(8)-N(5)-C(4)	117.5(9)
N(7)-C(15)	1.386(12)	C(10)-N(6)-C(16)	117.3(9)
N(8)-N(9)	1.359(10)	C(11)-N(7)-C(15)	117.9(9)

N(8)-C(18)	1.385(12)	N(9)-N(8)-C(18)	105.2(8)
N(9)-N(10)	1.323(10)	N(9)-N(8)-Cu(3)	121.9(6)
N(9)-Cu(2)#8	1.987(8)	C(18)-N(8)-Cu(3)	132.5(7)
N(10)-C(19)	1.376(12)	N(10)-N(9)-N(8)	113.3(7)
N(10)-Cu(1)#9	2.065(8)	N(10)-N(9)-Cu(2)#8	120.6(6)
C(1)-C(6)	1.411(13)	N(8)-N(9)-Cu(2)#8	126.0(6)
C(1)-C(2)	1.441(13)	N(9)-N(10)-C(19)	105.8(7)
C(2)-C(3)	1.380(13)	N(9)-N(10)-Cu(1)#9	127.8(6)
C(3)-C(4)	1.407(14)	C(19)-N(10)-Cu(1)#9	126.1(7)
C(3)-H(3)	0.9500	N(1)-C(1)-C(6)	131.2(9)
C(4)-C(5)	1.444(14)	N(1)-C(1)-C(2)	106.3(9)
C(5)-C(6)	1.393(13)	C(6)-C(1)-C(2)	122.5(9)
C(6)-H(6)	0.9500	C(3)-C(2)-N(3)	132.0(9)
C(7)-C(8)	1.440(15)	C(3)-C(2)-C(1)	122.0(10)
C(7)-C(12)	1.531(15)	N(3)-C(2)-C(1)	106.0(8)
C(8)-C(9)	1.525(16)	C(2)-C(3)-C(4)	116.8(10)
C(9)-C(21)	1.351(18)	C(2)-C(3)-H(3)	121.6
C(9)-C(10)	1.530(15)	C(4)-C(3)-H(3)	121.6
C(9)-C(22)	1.702(19)	N(5)-C(4)-C(3)	119.0(10)
C(10)-C(11)	1.393(15)	N(5)-C(4)-C(5)	120.4(9)
C(11)-C(12)	1.532(14)	C(3)-C(4)-C(5)	120.6(9)
C(12)-C(13)	1.521(16)	N(4)-C(5)-C(6)	116.6(9)
C(12)-C(14)	1.56(2)	N(4)-C(5)-C(4)	119.9(9)
C(13)-H(13A)	0.9800	C(6)-C(5)-C(4)	123.4(9)
C(13)-H(13B)	0.9800	C(5)-C(6)-C(1)	114.6(9)
C(13)-H(13C)	0.9800	C(5)-C(6)-H(6)	122.7
C(14)-H(14A)	0.9800	C(1)-C(6)-H(6)	122.7
C(14)-H(14B)	0.9800	N(4)-C(7)-C(8)	122.3(10)
C(14)-H(14C)	0.9800	N(4)-C(7)-C(12)	117.8(10)
C(15)-C(20)	1.389(13)	C(8)-C(7)-C(12)	119.3(10)
C(15)-C(16)	1.443(13)	N(5)-C(8)-C(7)	121.1(10)
C(16)-C(17)	1.399(13)	N(5)-C(8)-C(9)	114.0(10)
C(17)-C(18)	1.363(13)	C(7)-C(8)-C(9)	124.6(10)
C(17)-H(17)	0.9500	C(21)-C(9)-C(8)	119.4(12)
C(18)-C(19)	1.393(13)	C(21)-C(9)-C(10)	116.9(12)
C(19)-C(20)	1.418(14)	C(8)-C(9)-C(10)	111.8(11)
C(20)-H(20)	0.9500	C(21)-C(9)-C(22)	107.0(14)
C(21)-H(21A)	0.9800	C(8)-C(9)-C(22)	96.5(9)
C(21)-H(21B)	0.9800	C(10)-C(9)-C(22)	101.0(10)
C(21)-H(21C)	0.9800	N(6)-C(10)-C(11)	124.0(10)
C(22)-H(22A)	0.9800	N(6)-C(10)-C(9)	113.1(11)
C(22)-H(22B)	0.9800	C(11)-C(10)-C(9)	122.9(10)
C(22)-H(22C)	0.9800	N(7)-C(11)-C(10)	121.5(10)
		N(7)-C(11)-C(12)	115.4(10)
		C(10)-C(11)-C(12)	123.0(10)
		C(13)-C(12)-C(7)	112.4(9)
		C(13)-C(12)-C(11)	110.5(10)

C(7)-C(12)-C(11)	113.6(9)
C(13)-C(12)-C(14)	102.7(11)
C(7)-C(12)-C(14)	108.9(10)
C(11)-C(12)-C(14)	108.1(9)
C(12)-C(13)-H(13A)	109.5
C(12)-C(13)-H(13B)	109.5
H(13A)-C(13)-H(13B)	109.5
C(12)-C(13)-H(13C)	109.5
H(13A)-C(13)-H(13C)	109.5
H(13B)-C(13)-H(13C)	109.5
C(12)-C(14)-H(14A)	109.5
C(12)-C(14)-H(14B)	109.5
H(14A)-C(14)-H(14B)	109.5
C(12)-C(14)-H(14C)	109.5
H(14A)-C(14)-H(14C)	109.5
H(14B)-C(14)-H(14C)	109.5
N(7)-C(15)-C(20)	118.7(9)
N(7)-C(15)-C(16)	119.8(9)
C(20)-C(15)-C(16)	121.5(9)
N(6)-C(16)-C(17)	120.0(9)
N(6)-C(16)-C(15)	119.4(9)
N(8)-C(18)-C(19)	107.1(9)
N(10)-C(19)-C(18)	108.6(9)
N(10)-C(19)-C(20)	128.6(9)
C(18)-C(19)-C(20)	122.8(9)
C(15)-C(20)-C(19)	115.4(9)
C(15)-C(20)-H(20)	122.3
C(19)-C(20)-H(20)	122.3
C(9)-C(21)-H(21A)	109.5
C(9)-C(21)-H(21B)	109.5
H(21A)-C(21)-H(21B)	109.5
C(9)-C(21)-H(21C)	109.5
H(21A)-C(21)-H(21C)	109.5
H(21B)-C(21)-H(21C)	109.5
C(9)-C(22)-H(22A)	109.5
C(9)-C(22)-H(22B)	109.5
H(22A)-C(22)-H(22B)	109.5
C(9)-C(22)-H(22C)	109.5
H(22A)-C(22)-H(22C)	109.5
H(22B)-C(22)-H(22C)	109.5

Symmetry transformations used to generate equivalent atoms:

```
#1 -x+2,y,-z+1/2 #2 x+1/2,y+1/2,z #3 -x+3/2,y+1/2,-z+1/2
#4 x,-y+1,z-1/2 #5 x+1/2,-y+1/2,z-1/2 #6 -x+1,y,-z+3/2
#7 x,-y+1,z+1/2 #8 x-1/2,-y+1/2,z+1/2 #9 x-1/2,y-1/2,z
```

7. UV/vis spectroscopy

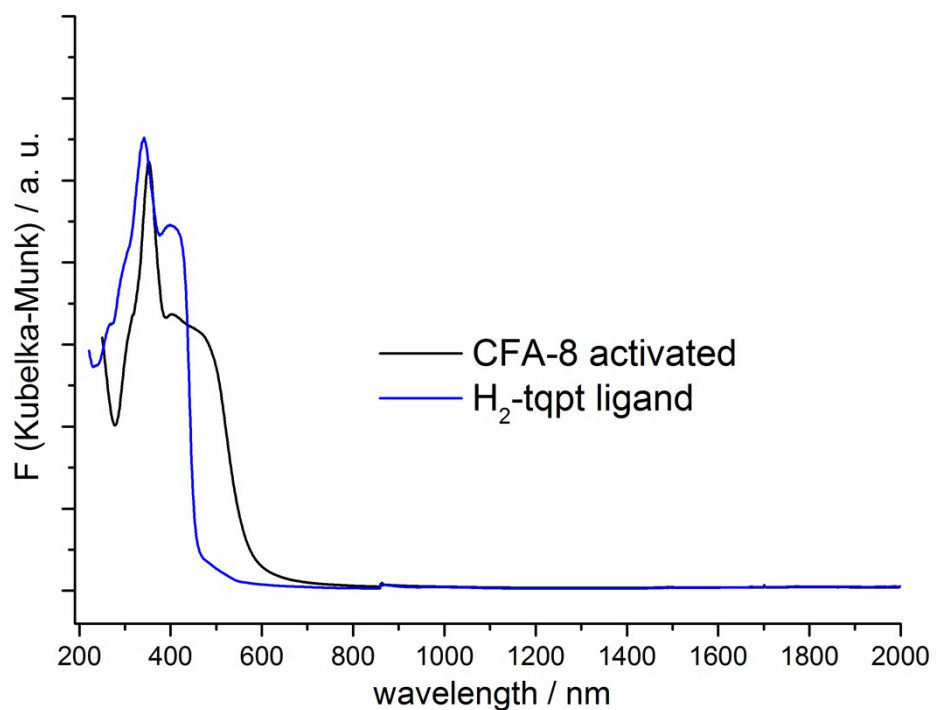


Figure S 10 Diffuse reflectance UV/vis-NIR spectra of CFA-8 and the organic H₂-tqpt ligand.

8. Variable temperature synchrotron powder diffraction measurements

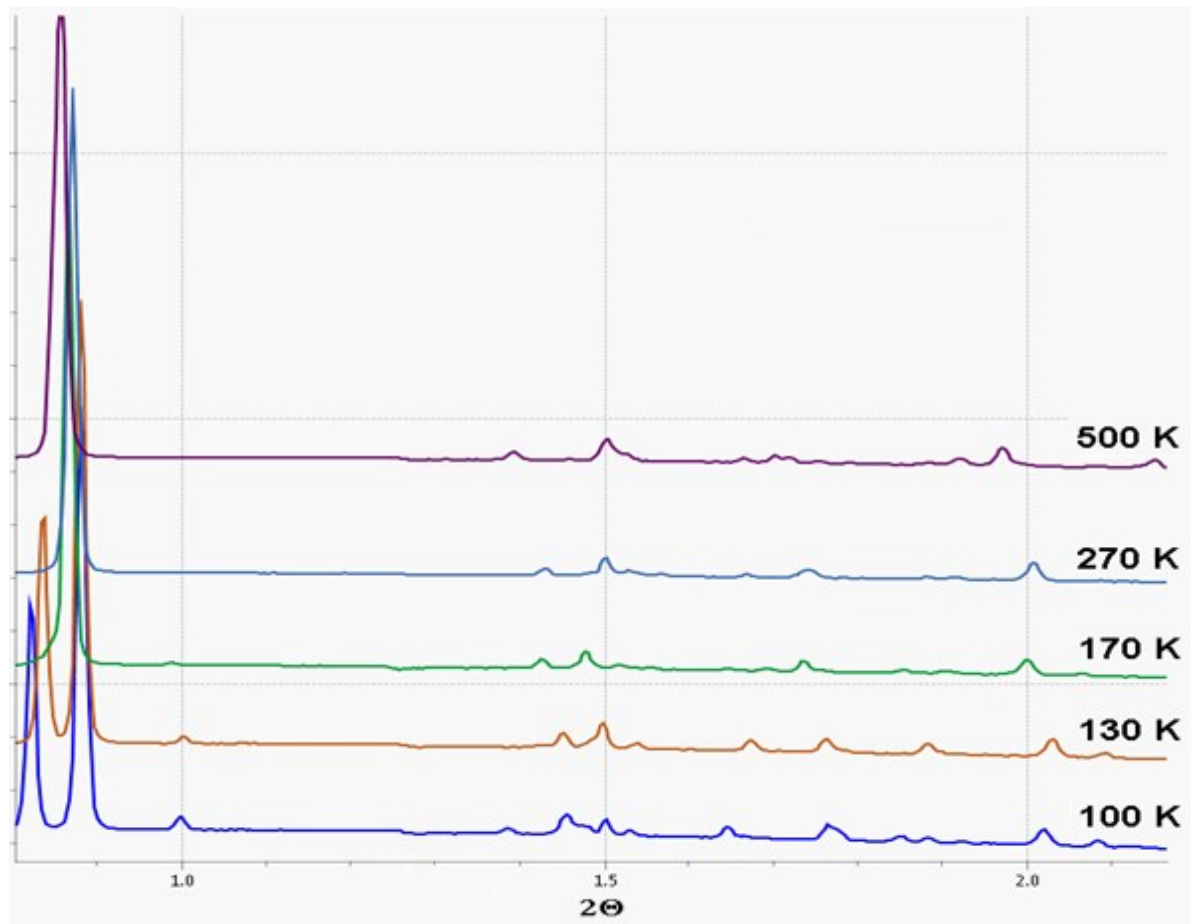


Figure S 11 Variable temperature synchrotron powder diffraction of evacuated CFA-8 at 500 K, 270 K, 170 K, 130 K, and 100 K (sample was kept under deep vacuum during measurements). Splitting of strongest peak between $2\theta = 0.8^\circ$ and $2\theta = 0.9^\circ$ into two peaks as well as appearing of small peak around $2\theta = 1^\circ$ can indicate temperature induced changing to the structure with triclinic symmetry.

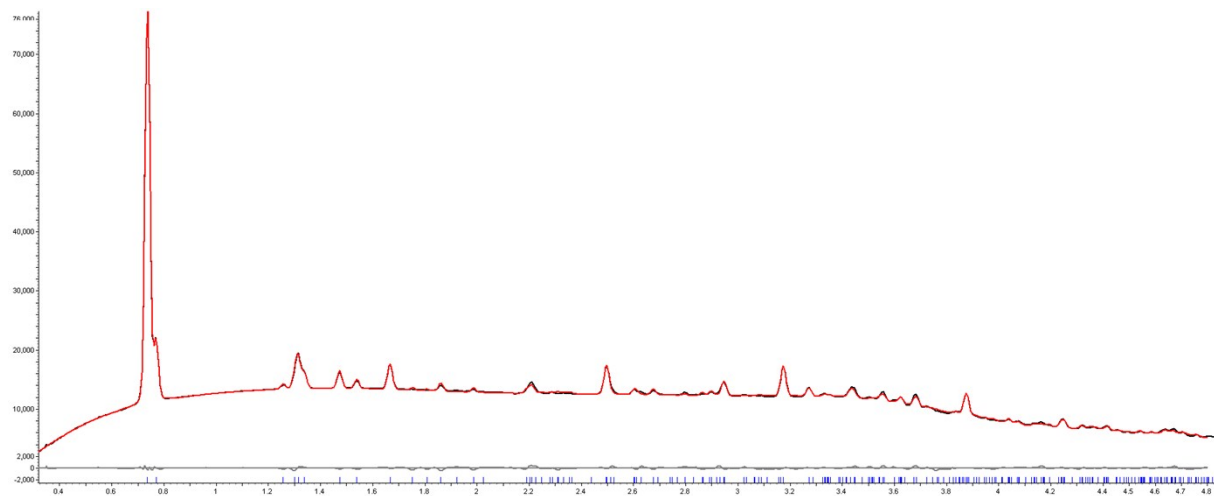


Figure S 12 Rietveld refinement of the XRPD pattern of CFA-8 under exposure by CO gas (100 kPa, 100 K). Black and red lines represent observed and calculated patterns, respectively, with peak markers and the difference plot shown at the bottom.

9. Structure solution and refinement from powder diffraction data of the narrow-pore phase of CFA-8 with adsorbed CO molecules.

Table S5 Crystal and experimental data for the CFA-8 with adsorbed molecules of CO gas (100 kPa, 100 K).

CFA-8·10 CO	
Formula weight	1465.32
Temperature (K)	100(2)
Wavelength (Å)	0.207
Crystal system	monoclinic
Space group	<i>C</i> 2/c (no. 15)
Unit cell dimensions (Å)	a = 30.866(4) Å b = 18.881(1) Å c = 10.851(2) Å β = 93.29(2) °
Volume	6313.5(12) Å ³
Z	4
Density (calculated) (g/cm³)	1.409
Theta range (°)	0.2 to 5
GooF	2.006
R_p	1.35
R_{wp}	1.83

10. In situ XRPD measurements under CO₂ and 80 % humidity

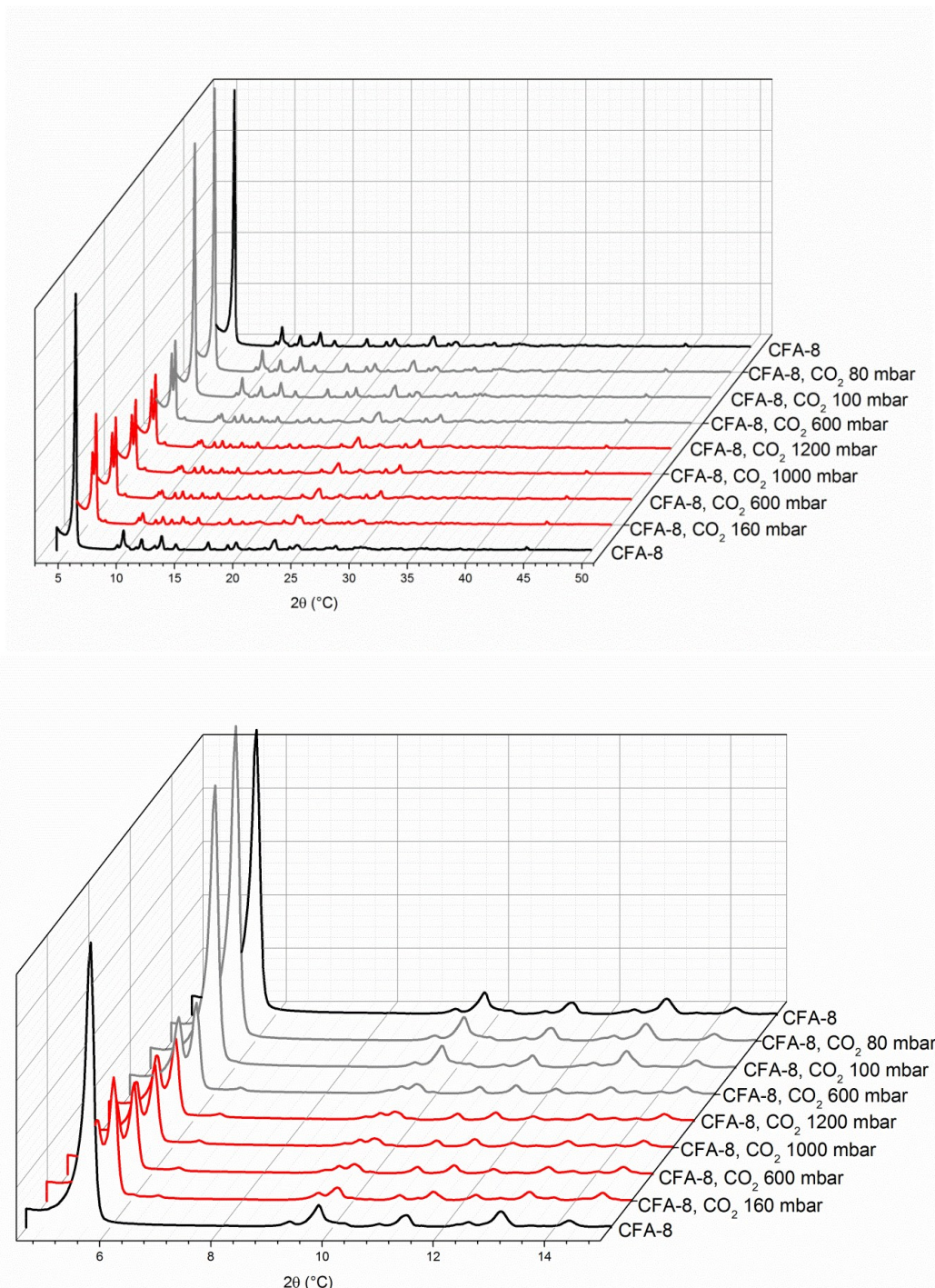


Figure S 13 *In situ* XRPD plots of CFA-8 measured at -78.5 °C in vacuum (black line) and under increasing CO₂ pressure (red lines) and decreasing CO₂ pressure (grey lines).

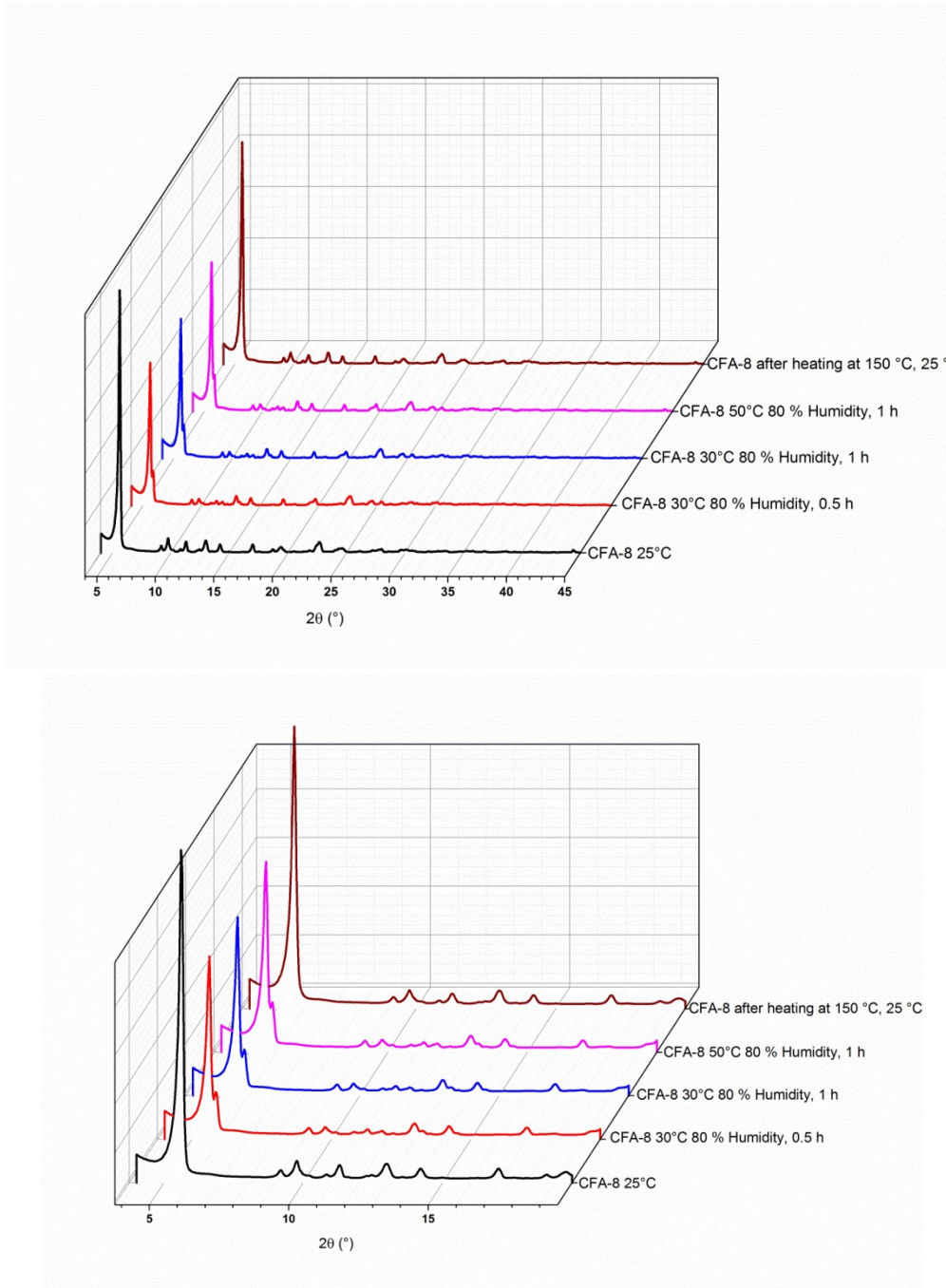


Figure S 14 *In situ* XRPD plots of CFA-8 measured at 80 % humidity.